# Strange Metals and SYK models

Jaychandran Padayasi*

*Department of Physics,*

*The Ohio State University, Columbus.*

(Dated: April 14, 2021)

**CONTENTS**



* padayasi.1@osu.edu

## I. INTRODUCTION

The Sachdev-Ye-Kitaev (SYK) model was introduced as the Sachdev-Ye model in 1993 [1] as a simple, random $SU(M)$ magnetic model to study spin glasses. It was revived in 2015 [2] by Kitaev's famous lecture where a mapping was made from a simpler version of the model to gravity in one space and one time dimension. Since then, the mapping to the gravitional model has been established on a firmer footing [3].

In this paper, we focus on the utility of SYK models to explain the phenomenology of *strange metals* found across condensed matter systems [4]. Strange metals are strongly correlated phases of matter first discovered in the context of cuprate high-$T_c$ superconductors. They show linear-in-$T$ resistivity in the low temperature limit, and indicate a lack of Landau quasiparticles. The universality of the temperature-scaling in transport has led to the idea of a "Planckian metal" in which momentum relaxation processes are independent of anything but the temperature and the Planck's constant $\hbar$. A similar bound is famous in black hole physics as black holes are maximally chaotic (disperse information as fast as it is physically possible). Hence, it is natural to study SYK models in this context. They are a family of exactly solvable models with non-Fermi liquid features (and linear-in-$T$ transport) with well-established connections to a dual gravitational model.

The organization of the rest of this paper is as follows: in Sec II we review experimental literature and the associated phenomenology of strange metals. We also discuss why SYK models inspire hope in solving the puzzle of strange metals. In Sec III, we introduce the reader to two versions of the classic quantum-dot SYK model augmented with two approaches to obtaining the Green's function analytically in the strong coupling and low-temperature limit. Next, Sec IV A and Sec IV B, we discuss two proposals for the experimental realization of SYK physics. The design outlined in IV B (graphene flake in a magnetic field) is possible to fabricate with current technology and offers an example of the microscopic interaction effects that are *ab initio* of the form of SYK. Finally, we conclude with the cautious optimism that future studies will continue to chip at the problem, and that SYK physics will play a significant role in our understanding of strange metals.

## II. STRANGE METAL PHENOMENOLOGY

What is so *strange* about strange metals, i.e. how do they differ from regular metals? What are the different theoretical models one could build to explain the anomalies in the experiments? In this section, we give a bird's eye view of the current debate on such questions to introduce the bizarre world of strange metals. We summarise the various experimental and theoretical phenomenology behind the phase of matter called strange metals.

### A. Semiclassical transport in metals

Classic solid state physics defines *metals* as materials that possess a continuous density of states around the Fermi energy (or equivalently, the chemical potential at $T = 0$). They have mobile charge carriers at low temperatures because they have arbitrarily close low-energy excitations in their spectra. Transport in metals is very well-described by the scattering of *quasiparticles*, such as screened electrons or electron-hole pairs. For the quasiparticle approximation to hold, these excitations must have a long lifetime; $\tau_{qp}^{-1} \sim T^d$ with $d > 1$ in the low-temperature limit. The quantum Boltzmann equation (1) describes transport in the semiclassical picture of quasiparticles undergoing a random walk, scattering off impurities/quasiparticles or lattice vibrations. It is written in terms of the dynamic number density $f(r, k, t)$ of electrons/quasiparticles in classical phase space:

$$\partial_t f + \mathbf{v}(\mathbf{k}) \cdot \nabla_r f + \frac{1}{\hbar}\mathbf{F} \cdot \nabla_k f = (\partial_t f)_{\text{coll}}. \tag{1}$$

The collision integral (the only term on RHS) in Eq. (1) in semiclassical transport applications is modeled via a *relaxation time approximation*:

$$(\partial_t f)_{\text{coll}} = \frac{f(k) - f_0(k)}{\tau_{\text{tr}}(k)} \tag{2}$$

which reflects the idea that each momentum wavevector relaxes independently. Notice that the time which enters Eq. (2), $\tau_{\text{tr}}$ is different than the quasiparticle lifetime $\tau_{\text{qp}}$ because the transport lifetime excludes small-angle collisions that are inefficient at relaxing the momentum. Solving the transport Eq. (1) after linearizing, for a parabolic band of effective mass $m^*$ yields a Drude-like result for the conductivity

$$\sigma = \frac{ne^2\tau_{\text{tr}}}{m^*} \tag{3}$$

Thus, the temperature dependence of resistivity $\rho = \sigma^{-1}$ is due to $\tau_{\text{tr}}$. Heuristically, we can consider different scattering processes that relax momentum [5]:

- Scattering off impurities: the time between collisions only depends on the density of atomic impurities $n_i = N_i/V$ and therefore is independent of temperature;

  $$\tau^{-1}_{\text{tr;imp}}(T) = c$$

  where $c$ is a constant.

- Scattering off other electrons/quasiparticles: The scattering rate $\Gamma = \tau^{-1}_{\text{tr;ee}}$ for such processes can be calculated from Fermi's golden rule. At low temperatures, the width of the Fermi-Dirac distribution $n_F(k)$ is of the order of $T$. Thus, the scattering rate is proportional to $n_F(k_i)n_F(k_f) \approx T^2$ where $k_i$ and $k_f$ are the initial and final momenta of the quasiparticles. Thus,

  $$\tau^{-1}_{\text{tr;ee}}(T) = bT^2.$$

- Scattering off phonons: Phonons are quanta of lattice vibrations whose wavelengths cannot be smaller than the lattice spacing. Hence, their energies are limited by a characteristic temperature scale called the *Debye temperature* $\Theta_d$. For $T \gg \Theta_d$, the electron-phonon scattering is dominated by phonons of energy $\Theta_d$, and the transport lifetime scales as

  $$\tau^{-1}_{\text{tr;e-ph}}(T) = AT.$$

  For $T \ll \Theta_d$, the average energy of the phonons is $\sim T$. This gives a transport lifetime scaling of

  $$\tau^{-1}_{\text{tr;e-ph}}(T) = aT^5$$

  which goes by the name of Bloch's law in literature.

Combining all of the processes mentioned above, the resistivity for low temperatures $T \ll \Theta_d$ depends on temperature as

$$\rho = \tilde{c} + \tilde{b}T^2 + \tilde{a}T^5. \tag{4}$$

Note that at the lowest temperatures, resistivity scales atleast as $T^2$ depending on whether electron-electron or electron-phonon scattering processes are dominant. At higher temperatures, electron-phonon scattering is dominant and we get

$$\rho = AT. \tag{5}$$

These results are the hallmark of semiclassical transport, and signify the existence of a Fermi liquid phase with well-defined quasiparticles.

### B. Anomalous transport in strange metals

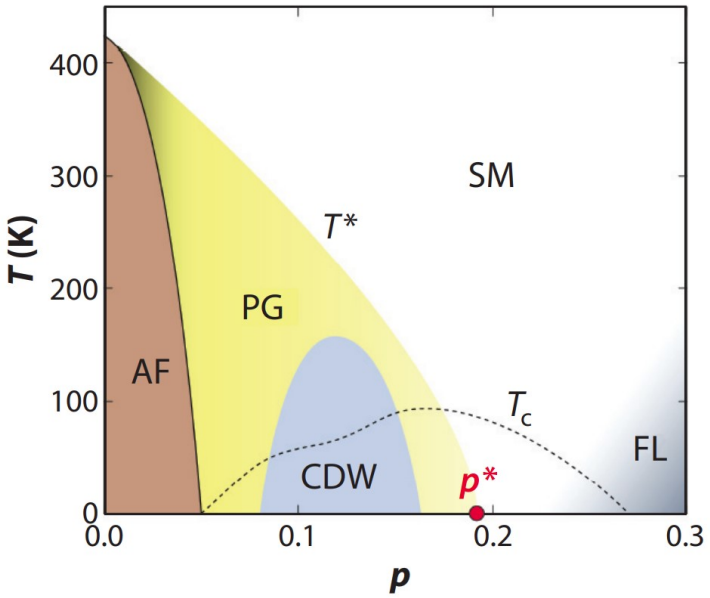


FIG. 1: Phase diagram of hole-doped cuprates, in the plane of doping and $T$ (reproduced from [4]). The various phases labeled in the diagram are: Doped Mott-insulator with Antiferromagnetic order (AF), Pseudogap state (PG), Charge-density wave phase (CDG) and the Strange Metal phase (SM).

A *strange metal* is characterised by anomalous scaling in transport and thermodynamic coefficients. In particular, resistivity in strange metals scales linearly in temperature even at very low temperatures $\rho(T) \sim T$ (Fig 2). The electron-phonon scattering process gives a linear in $T$ resistivity at high-temperatures in all metals, but in these materials the property persists to temperatures much lower than the Debye temperature (although there are some that recover $\sim T^2$ dependence at lower temperatures, such as Strontium Ruthenate [6]). On the high-$T$ side, the quasiparticle picture is ill-defined if the quantum mechanical mean free path $l = v_F \tau_{\rm qp}$ is smaller than its momentum $k_F$. Thus, we have $k_F l > 1$ which leads to the Mott-Ioffe-Regel limit as an upper bound at which resistivity must saturate at high

temperatures [7]:

$$\rho < \frac{h}{e^2 k_F^{d-2}}. \tag{6}$$

Strange metals violate this limit as well, with resistivity increasing linearly beyond the bound without saturation. The term strange metal was first used to describe a phase discovered in cuprate superconductors near optimal doping [4] (see Fig 1). Since then, strange metal behavior has been observed in Strontium Ruthenate $Sr_3Ru_2O_7$ [6] and in other systems like pnictides, magic-angle graphene [8] and ultracold atoms [9]. Transport in the strange metal phase is believed to not originate from any of the conventional processes we discussed above. Moreover, photoemission data [10] show no well-defined quasiparticles in some of the materials, leading to the conjecture that strange metals are *non-Fermi liquids*, often used synonymously to denote the same set of properties.

An even more surprising empirical observation is the *Planckian dissipation* in strange metals [11]. The low-temperature resistivity of many different families of cuprate strange metals seem to follow (as discussed) $\rho \approx \rho_0 + AT$ with an universal slope $A$! It suggests that the mechanism that explains the strange metal phase cannot depend on the specifics of the material like the size/shape of the Fermi surface, the interaction strength, etc. The universality is captured by the transport lifetime behavior

$$\frac{1}{\tau_{\text{tr}}} = \alpha \frac{k_B T}{\hbar} \tag{7}$$

with $\alpha \approx 1$ among a wide variety of materials.

There are various candidates for theories of strange metal phenomena. Given the diversity in the defining phenomenology, it is likely that the non-Fermi liquid behavior in different systems is realized by more than one of these mechanisms. Some of the candidates that we will not cover in this paper are (see [12]):

- A generalization of electron-phonon scattering: a bosonic order parameter coupled to a Fermi surface
- Interaction-driven phase transitions, such as the Mott transition, that may possess a critical Fermi surface but (by definition) no quasiparticles

Finally, SYK models provide yet another perspective in which strange metals may be realized. There are several cogent arguments as to why SYK models (and extensions thereof) might fit the bill for a universal theory of strange metals.

- It is a strongly-correlated, highly-disordered quantum dot. We know that correlation plays a crucial role in the physics of cuprates but it is yet to be seen if disorder is relevant.

- It is also an exactly soluble theory in certain limits even though it has no well-defined quasiparticles, which makes it ripe for a rich theoretical exploration of non-Fermi liquids.

- Various higher-dimensional extensions of SYK models exist that reproduce linear-in-$T$ resistivity over a wide range of temperatures.

- SYK saturates the bound on quantum chaos at low temperatures, dissipating information as quickly as possible. It is believed that such a mechanism explains the universality/Planckian dissipation of strange metals.

As we have shown, the field of strange metal physics is an active research area, with great deal of effort being spent on all the three aspects: experiments, numerics and theory. If it is indeed discovered that linear-in-$T$ resistivity is generic in strongly correlated materials and that disorder plays a crucial role in defining the phase, it is likely that holographic models such as the SYK will prevail as the accepted theory for the same.

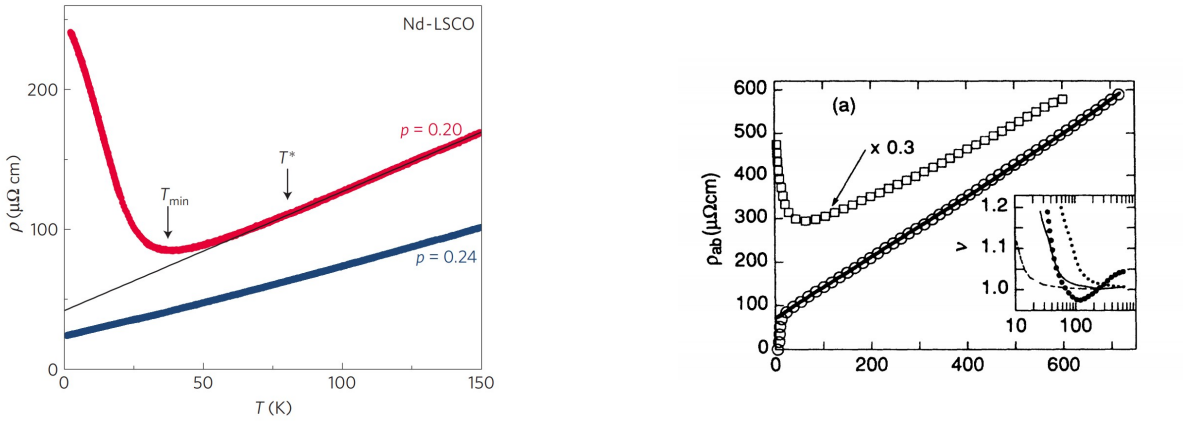


FIG. 2: **Strange metal behavior in cuprates:** The cuprates when doped into their superconducting phase show linear-in-$T$ resistivity over a wide range of temperatures (possibly to $T = 0$). Shown here are two examples, the left figure from [13] in Neodymium doped LSCO and the right from [14] in Bi-2201. Both show that the non-superconducting phase does not show strange metal behavior.

## III. SOLVABLE LIMITS OF THE SYK MODEL

Much of the interest in SYK models is because of their solvability. In what follows, we introduce two different versions of the model, with Majorana and complex fermions, and show various generalizations that one could make. SYK in its original version is defined as a zero-dimensional quantum system with no spatial structure. We reproduce classic calculations in certain useful limits and discuss the emergent symmetries.

### A. Diagrammatic method

The Sachdev-Ye-Kitaev model is a rare example of an exactly solvable model that is both disordered and strongly correlated. Here we present the diagrammatic solution of the simplified Majorana fermion model introduced by Kitaev. The details of this technique are explicitly worked out in [15] and [3]. The model is usually presented as a random all-to-all four-fermion interaction but in this calculation, we will work with a $q$-fermion interaction term ($q$ even) because later we will be looking at a model which has both $\text{SYK}_2$ ($q = 2$) and $\text{SYK}_4$ ($q = 4$) regimes. Consider the interacting Hamiltonian with $N$ Majorana fermions

$$H = i^{q/2} \sum_{i_j=1}^{N} J_{i_1 i_2 \ldots i_q} \chi_{i_1} \chi_{i_2} \cdots \chi_{i_q} \tag{8}$$

where the sum runs over distinct indices $i_1, i_2, \ldots i_q$. The couplings are assumed to be random, independent variables drawn from a Gaussian distribution with zero mean and

$$\overline{J^2_{i_1 i_2 \ldots i_q}} = \frac{J^2 (q-1)!}{N^{q-1}}. \tag{9}$$

The Majorana fermions are Hermitian operators that satisfy the usual anti-commutation relations,

$$\{\chi_i, \chi_j\} = \delta_{ij}. \tag{10}$$

It follows that the rank-$q$ tensor of couplings $J_{i_1 i_2 \ldots i_q}$ is totally anti-symmetric. It is useful to note the following identity which lets us disorder average over products of vertices:

$$\overline{J_{i_1 i_2 \ldots i_q} J_{j_1 j_2 \ldots j_q}} = \frac{J^2 (q-1)!}{N^{q-1}} \sum_{\sigma} \text{sgn}[\sigma] \prod_{n=1}^{q} \delta_{i_n, \sigma(j_n)}. \tag{11}$$

The sum runs over all possible permutation of the indices $\sigma$. This messy sum simply accounts for anti-symmetry; it finds indices which are the same up to an permutation and then sets

their average as the variance in Eq. (9). In the $N \to \infty$ limit, we will only need the highest order term in the sum as can be shown by an explicit calculation for the $q = 4$ case;

$$\sum_{k,l,m} \overline{J_{iklm} J_{jklm}} = \frac{3! J^2}{N^3} \sum_{k,l,m} (\delta_{ij}\delta_{kk}\delta_{ll}\delta_{mm} - \delta_{ik}\delta_{kj}\delta_{ll}\delta_{mm} + \ldots)$$
$$= \frac{3! J^2}{N^3} \left( N^3 \delta_{ij} + \mathcal{O}(N^2) \right) = 3! J^2 + \mathcal{O}\left(\frac{1}{N}\right). \quad (12)$$

*Green's functions*

Let us consider the time-ordered propagator for the SYK Majoranas in imaginary time:

$$G_{ij}(\tau_1, \tau_2) = \langle \mathbb{T}_\tau \chi_i(\tau_1) \chi_j(\tau_2) \rangle \quad (13)$$

The free propagator for the Majorana fermions maybe found from the equation-of-motion of the non-interacting Lagrangian

$$\mathcal{L}^{(0)} = \frac{1}{2} \sum_j \chi_j \partial_\tau \chi_j \quad (14)$$

and the anti-commutation relations. In Matsubara technique, it is

$$G^{(0)}_{ij}(i\omega_n) = -\frac{\delta_{ij}}{i\omega_n} \quad (15)$$

where $\omega_n = (2n+1)\frac{\pi}{\beta}$ and $n \in \mathbb{Z}$.

The full Green's function can then be expanded as usual in terms of interaction vertices and free propagators. However, we must also disorder average over the couplings. The disorder averaging connects two distinct vertices, as all averages of even number of vertices can be broken down into the two-coupling average by means of a Wick-like decomposition. The non-vanishing diagrams must also not contain loops; the interaction amplitudes are identically zero due to anti-symmetry $J_{i,i,i_3 \ldots i_q} = 0$.

Finally, we note that in the large-$N$ limit, the only diagrams that contribute to the connected part of the cluster expansion are the "melonic" diagrams like in Fig 3 for $\text{SYK}_4$. These involve an even number of vertices, separated into pairs which are connected between themselves by $q - 1$ free propagator lines and then coupled via disorder average. The dominance of such diagrams has been proved rigorously (see, for e.g. [16]), but it can also be understood via some heuristic arguments such as in [3]. Hereon, we will assume that this is the case.

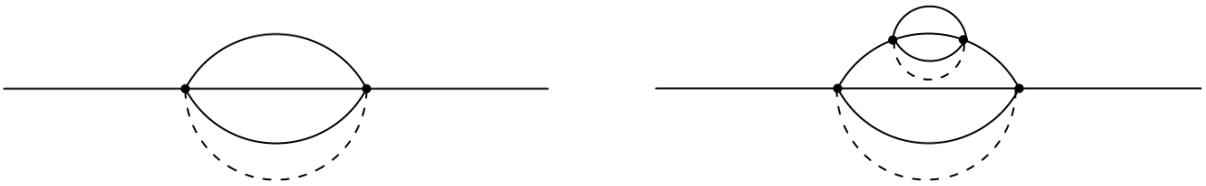

FIG. 3: Examples of melonic diagrams for $\mathrm{SYK}_4$.

The infinite family of melonic diagrams is easy to sum by writing a Schwinger-Dyson equation for the self-energy. In this case, the self-energy consists of all the one-particle irreducible diagrams, i.e., the melons themselves. As per Eq. (12), every dashed line contributes a factor of $J^2$ to the self-energy. Thus, the Schwinger-Dyson equations are:

$$G(i\omega_n)^{-1} = -i\omega_n - \Sigma(i\omega_n) \qquad \Sigma(\tau) = J^2 G(\tau)^{q-1} \tag{16}$$

The simplicity of Schwinger-Dyson (S-D) equations is testimonial to the solvability of the SYK model. It arises from the dominance of melonic diagrams in the large-$N$ limit, as discussed above. These equations can be solved numerically to self-consistency, starting from $G \approx G^{(0)}$.

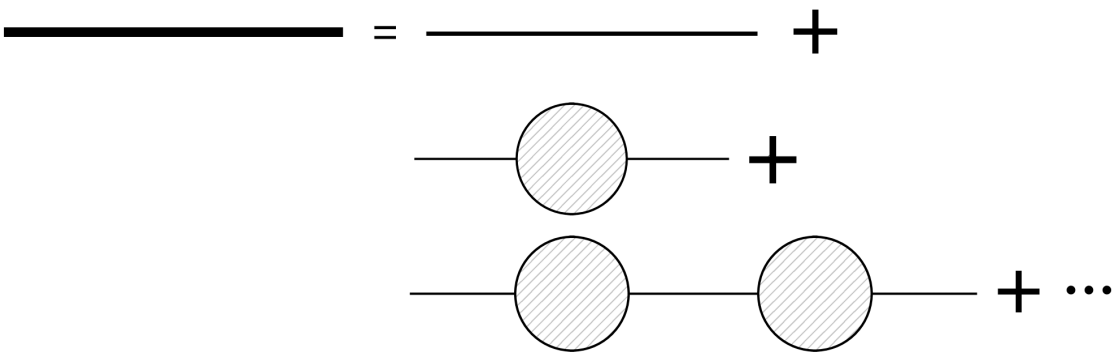

FIG. 4: Graphical representation of the Schwinger-Dyson equations (16). The thick line represents the full Green's function, the thin lines the free Green's function and the hatched blobs represent the self-energy.

*Conformal limit*

In the strong coupling limit ($\beta J \gg 1$), the Schwinger-Dyson Eqs. (16) have emergent conformal symmetry [2]. In this limit, it is safe to neglect the contribution from the free Green's function $i\omega_n$ in the first equation. Thus, we have

$$\int d\tau_3 \; G(\tau_1,\tau_3)\Sigma(\tau_3,\tau_2) = -\delta(\tau_1-\tau_2) \qquad \Sigma(\tau_1,\tau_2) = J^2[G(\tau_1,\tau_2)]^{q-1} \tag{17}$$

which are invariant under an arbitrary reparameterization of time

$$\tau \to \sigma = f(\tau)$$

given that the fields $\Sigma$ and $G$ are appropriately scaled as

$$G(\sigma_1,\sigma_2) = (f'(\tau_1)f'(\tau_2))^{\Delta} G(\tau_1,\tau_2) \qquad \Sigma(\sigma_1,\sigma_2) = (f'(\tau_1)f'(\tau_2))^{\Delta(q-1)}\Sigma(\tau_1,\tau_2). \tag{18}$$

The scaling dimension $\Delta$ can be read off from the first equation in Eqs. (17) as $\Delta = \frac{1}{q}$. It is remarkable that, starting from a microscopic model that was not symmetric, we have found a limit in which the conformal symmetry is *emergent*.

Once the conformal symmetry is established, it is easy to guess the form of $G(\tau_1,\tau_2)$ as a standard two-point function of a CFT with scaling dimension $\Delta$:

$$G_c(\tau) = \frac{b}{|\tau|^{2\Delta}}\mathrm{sgn}(\tau) \tag{19}$$

The conformal solution $G_c$ is only valid for $T = 0$, as it is not anti-periodic about a finite $\tau = \beta$. We obtain the finite temperature solution by the conformal transformation

$$\tau \to \sigma = \tan\frac{\tau\pi}{\beta},$$

$$G_c^{\beta}(\tau) = b\left(\frac{\pi}{\beta\left|\sin\frac{\pi\tau}{\beta}\right|}\right)^{2\Delta}\mathrm{sgn}(\tau). \tag{20}$$

In both of the solutions obtained above, the undetermined parameter $b$ is found by inserting the ansatz into Eqs. (17). The spectral function follows from the imaginary part of the Green's function and for low energies goes as $\rho(\omega) \sim 1/\sqrt{\omega}$, not lending itself to a quasiparticle interpretation.

*Entropy*

Another feature of the SYK model is that the zero-temperature entropy is non-zero and extensive in $N$. Specifically, for general $q$, the temperature-independent entropy $S_0$ is given as [15][2]

$$\frac{S_0}{N} = \frac{1}{2}\ln(2) - \int_0^{1/q} dx\ \pi \left(\frac{1}{2} - x\right) \tan \pi x \tag{21}$$

We see that, in the case of $q = 2$, where the SYK model is just a quadratic random hopping model, the integral exactly cancels out the constant and $S_0 = 0$. This disordered free fermion model admits a quasiparticle description, and thus cannot explain anomalous transport behavior by itself [17]. For higher-order couplings, the entropy $S/N$ approaches a constant value as $T \to 0$.

### B. Functional Integral method

The Schwinger-Dyson Eqs. (16) were historically first derived as the saddle point equations of a replicated action in a functional integral [1][18]. The technique presents a useful contrast to the diagrammatic method and puts the results on a firmer footing. Consider the $\text{SYK}_4$ model with complex spinless fermions instead of the Majoranas, so that they have a conserved $U(1)$ charge density $\mathcal{Q}$ [18],

$$H = \sum_{i,j,k,l=1}^{N} J_{ij;kl} c_i^\dagger c_j^\dagger c_k c_l - \mu \sum_{i=1}^{N} c_i^\dagger c_i \tag{22}$$

with complex couplings $J_{ij;kl}$ that are anti-symmetric about the exchange of indices on either sides of the semicolon and $J_{ij;kl} = J^*_{kl;ij}$. Let the complex variables have independent real and imaginary parts with zero meanand the same variance so that $\overline{|J_{ij;kl}|^2} = \frac{J^2}{4N^3}$ (following [19]).

To disorder average Eq. (22), we use the *replica trick*. Introducing $n$ copies of the system with the same disorder realization and averaging over them removes the quenched disorder but introduces interactions between the replicated copies. Next, using the formula

$$\overline{\ln(Z)} = \lim_{n\to 0} \frac{\overline{Z^n} - 1}{n}, \tag{23}$$

one can obtain the thermodynamic free-energy. Taking the replica limit has to be handled on a case-by-case basis, and no general proofs exist for the validity of the formula. Nevertheless,

it is widely used especially in the context of spin-glasses in which the SYK model was first introduced. For the complex $\mathrm{SYK}_4$ model, we will stop short of this step, as we will only be looking at the saddle-point equations of a *replica-diagonal solution*. The replicated partition function and its disorder average for the model Eq. (22) is defined as

$$Z^n = \mathrm{Tr}\ \mathbb{T}\ \exp\left[-\left(\int_0^\beta d\tau \sum_{i,a} c^\dagger_{ia}(\partial_\tau - \mu)c_{ia} + \sum_{i,j,k,l}\int_0^\beta d\tau d\tau' J_{ij;kl}\left[\sum_a c^\dagger_{ia}(\tau)c^\dagger_{ja}(\tau)c_{ka}(\tau')c_{la}(\tau')\right]\right)\right] \tag{24a}$$

$$\overline{Z^n} = \prod_{i,j,k,l}\int_{\mathbb{C}} dJ_{ij;kl}\ \left(\frac{N^3}{2\pi J^2}\right)\exp\left(-\frac{|J_{ij;kl}|^2 N^3}{2J^2}\right) Z^n. \tag{24b}$$

Executing the averages by completing the square (see, for e.g. [20]), we have the following replicated action

$$S[c] = \int_0^\beta d\tau\ \sum_{i,a} c^\dagger_{ia}(\partial_\tau - \mu)c_{ia} - \frac{J^2}{4N^3}\sum_{a,b}\int_0^\beta d\tau d\tau' \left|\sum_i c^\dagger_{ia}(\tau)c_{ib}(\tau')\right|^4 \tag{25}$$

where we have neglected terms which are not normal-ordered [18]. Now we can perform Hubbard-Stratonovich transformations to decouple the eight-fermion term. As the interaction term appears as a square of a real number ($\sim (|\mathcal{Q}|^2)^2$), we introduce the real field $Q_{ab}(\tau,\tau') = Q_{ba}(\tau,\tau')$ first to reduce it to a quartic term. Using the identity

$$\int \mathcal{D}Q\ \exp\left[-\sum_{a,b}\int_0^\beta d\tau d\tau'\ \frac{N^4}{J^4}Q^2_{ab} + \frac{2N^2 Q_{ab}}{J^2}\left|\sum_i c^\dagger_{ia}(\tau)c_{ib}(\tau')\right|^2\right] = n\ \exp\left(\int_0^\beta d\tau d\tau'\ \sum_{a,b}\left|\sum_i c^\dagger_{ia}(\tau)c_{ib}(\tau')\right|^4\right), \tag{26}$$

we get the effective Hubbard-Stratonovich action

$$S[Q,c] = \int_0^\beta d\tau\ \sum_{i,a} c^\dagger_{ia}(\partial_\tau - \mu)c_{ia} - \sum_{a,b}\int_0^\beta d\tau d\tau'\ \left(\frac{1}{2N}Q_{ab}\left|\sum_i c^\dagger_{ia}(\tau)c_{ib}(\tau')\right|^2 - \frac{N}{4J^2}Q^2_{ab}(\tau,\tau')\right). \tag{27}$$

Next, we introduce a complex field $P_{ab}(\tau,\tau')$ such that $P_{ab}(\tau,\tau') = P^*_{ba}(\tau',\tau)$ and repeat the

procedure to obtain

$$S[Q,P,c] = \int_0^\beta d\tau \ \sum_{i,a} c^\dagger_{ia}(\partial_\tau - \mu)c_{ia} + \sum_{a,b}\int_0^\beta d\tau d\tau' \ \left(\frac{N}{4J^2}Q^2_{ab} + \frac{N}{2}Q_{ab}|P_{ab}|^2 \right.$$
$$\left. -Q_{ab}P_{ba}(\tau',\tau)\sum_i c^\dagger_{ia}(\tau)c_{ib}(\tau')\right). \quad (28)$$

To obtain the saddle-point equations, we must vary the given action with respect to $P_{ba}$ first and then $Q_{ab}$ giving us, in the large-$N$ limit

$$P_{ab}(\tau,\tau') = \frac{1}{N}\left\langle \sum_i c^\dagger_{ia}(\tau)c_{ib}(\tau')\right\rangle \quad (29a)$$

$$Q_{ab}(\tau,\tau') = J^2|P_{ab}(\tau,\tau')|^2 \quad (29b)$$

Replica diagonal solutions to the classical equations of the form $P_{ab} = \delta_{ab}G(\tau'-\tau)$ can be easily identified with the Green's function of the fermions. Re-writing the quadratic part of the action as

$$S_{\text{quad}} = \int_0^\beta d\tau d\tau' \sum_{i,a,b} c^\dagger_{ia}(\tau)\left[\delta_{ab}\delta(\tau-\tau')(\partial_\tau - \mu) + (-Q_{ab}(\tau,\tau')P_{ba}(\tau',\tau))\right]c_{ib}(\tau') \quad (30)$$

we see that the self-energy of the fermions is given by the last term in the square brackets. Thus, we arrive at the same Schwinger-Dyson equations as before:

$$G(i\omega_n) = i\omega_n + \mu - \Sigma(i\omega_n) \qquad \Sigma(\tau) = -J^2G^2(\tau)G(-\tau) \quad (31)$$

For complex fermions, unlike the Majoranas, in the conformal limit we have in addition to the emergent time reparameterization symmetry also a $U(1)$ gauge symmetry.

## IV. PROPOSED REALIZATIONS OF SYK MODELS IN STRANGE METALS

Having looked in detail at the zero-dimensional SYK model, in this section we look at two specific approaches to closing the gap between the abstract but exact physics of SYK models to various anomalous measurements in strange metals. The first one, reviewed in Sec IV A and first proposed in [17] is a sample from the zoo of higher-dimensional extensions of the SYK that is promising because it reproduces exact scaling and has reasonably tractable numerics. On the other end of the spectrum, in Sec IV B, we review a recent work proposing how the strong all-to-all disordered interaction can arise in a physical system, namely a graphene flake with an irregular boundary.

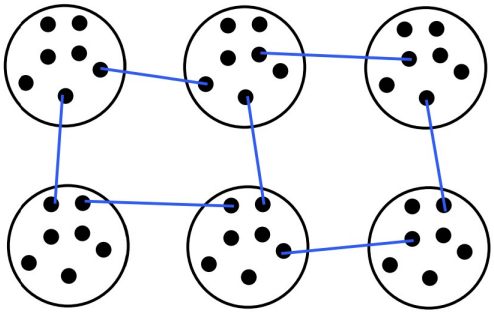

FIG. 5: A lattice of SYK islands: each island corresponds to a different flavor of fermion with its own set of random Gaussian couplings (taken from [21]).

### A. Crossover from Fermi liquid to non-Fermi liquid regime

The general paradigm for extending the SYK island to higher dimension is to consider a lattice of SYK islands, each being independent of the others, with some kind of hopping term between them as in Fig 5. The lattice index plays the role of a flavor index here. The $N$ fermions that reside on a single site are usually all-to-all coupled as in the usual $\text{SYK}_4$, and hopping between different sites varies among different proposals depending on what symmetries one wants to preserve in the microscopic model. In the model proposed in [17], the hopping itself is random, like a hopping version of $\text{SYK}_2$. Consider such an array of complex spinless fermions generically in $d$-dimensions

$$H = \sum_x \sum_{i,j,k,l} J_{ij;kl,x} c^\dagger_{ix} c^\dagger_{jx} c_{kx} c_{lx} + \sum_{\langle xx' \rangle} \sum_{i,j} t_{ij,x,x'} c^\dagger_{ix} c_{jx'} - \mu \sum_{i,x} c^\dagger_{ix} c_{ix} \tag{32}$$

where $J_{ij;kl,x}$ follow the same Gaussian distribution as in Sec III B and all the distributions are independent of the lattice site label $x$. Let the $\text{SYK}_2$ hoppings $t_{ij,x,x'} = t^*_{ji,x',x}$ be also Gaussian distributed with a variance $\overline{t^2_{ij,x,x'}} = T^2/N$. To average over disorder, we employ the key insight that up to $1/N$ order, the only diagrams that contribute to the replicated partition function average $\overline{Z^n}$ are replica diagonal ones [22]. Therefore we can consider the disorder-free action

$$S = \sum_x \int_0^\beta d\tau \; c^\dagger_{ix}(\tau)(\partial_\tau - \mu) c_{ix}(\tau) - \int_0^\beta d\tau_1 d\tau_2 \left( \sum_x \frac{J^2}{4N^3} \left| \sum_i c^\dagger_{ix}(\tau_1) c_{ix}(\tau_2) \right|^4 + \sum_{\langle xx' \rangle} \frac{T^2}{N} \left| \sum_i c^\dagger_{ix}(\tau_1) c_{ix'}(\tau_2) \right|^2 \right) \tag{33}$$

This model describes a crossover from a $SYK_4$ phase to a Fermi liquid $SYK_2$-like phase. As the individual terms are invariant with respect to time reparameterization, we expect the phases in the system to be described by fixed points with respect to this emergent scaling symmetry. Consider the non-Fermi liquid phase, with $J \gg T$. If we scale time as $\tau \to b\tau$ and keep $J$ invariant, we find the scaling dimensions of the fermion fields to be $\Delta = 1/4$ as expected. Clearly, the hopping rescales to $T^2 \to bT^2$ and is a relevant perturbation from this "fixed point". At the same time, starting from the hopping-dominant regime $T \gg J$ under the same time reparameterization, the fermion field would take their $SYK_2$ scaling dimension of $\Delta = 1/2$ lending the four-fermion term irrelevant ($J^2 \to J^2/b$). Working in the limit of $J \gg T$, we can define an energy scale $E_c = T^2/J$ that describes a crossover in Eq. (33) due to the relevant $SYK_2$ coupling. Thus, the key feature of the model is that in the low temperature limit $\beta \gg E_c$ one recovers some kind of Fermi liquid behavior. This is evident in the entropy calculations in [17] reproduced in Fig 6a. As we know, the $SYK_4$ model has an extensive zero-temperature entropy, whereas for a Fermi liquid we expect $S/N \to 0$. In the figure, the numerical calculation of entropy for different values of $T/J$ seem to interpolate between the $SYK_4$ limit for $(\beta E_c)^{-1} \gg 1$ and the $SYK_2$ limit for $(\beta E_c)^{-1} \ll 1$ where $T$ is the temperature. It also shows that our back-of-the-envelope calculation is impervious to the relative strength of the couplings $T/J$ so long as $J > T$ because all the curves collapse to the solid curve.

*Resistivity and Thermal conductivity*

To calculate transport in the model Eq. (32), one must shift to the real-time formulation. The electrical conductivity is obtained by looking at the variation of the saddle-point solutions to a $U(1)$ phase fluctuation $G \to Ge^{-i\phi}$, getting an effective low-energy action for the fields $\phi$ and solving for the density-density correlator. The thermal conductivity can be obtained by a similar process but by introducing time translations $t \to t + \epsilon$ instead. The procedure is detailed in [17] and its supplement wherein the authors also use some tricks specific to this formulation and problem.

The end result of the mental gymnastics is to verify the crossover in transport coefficients. The resistivity and thermal conductivity collapse to universal functions of the crossover energy $E_c$ and recover both limits. For example, for $T \gg E_c$ it is found that

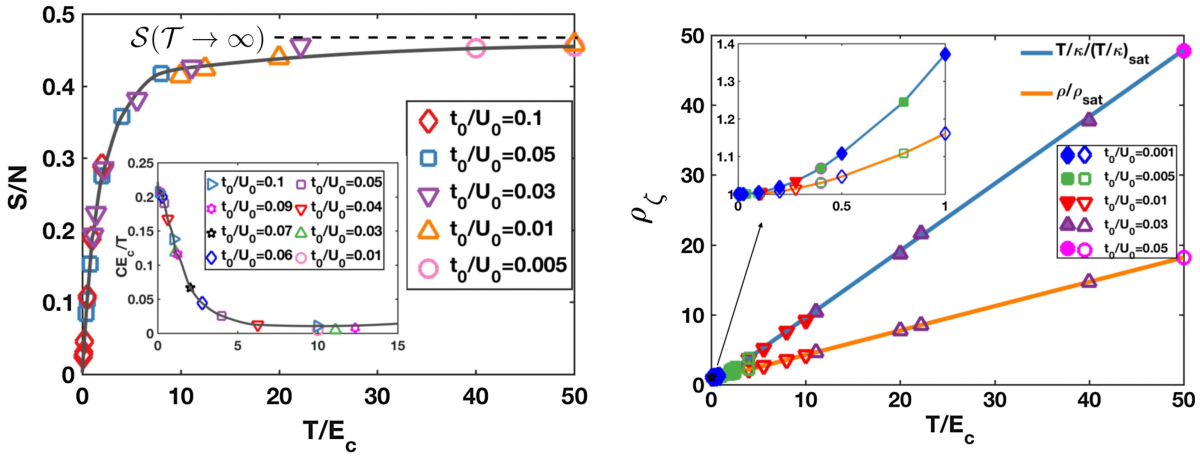


(a) (b)

FIG. 6: **Entropy and transport in Eq. (32)**: Numerical results taken from [17] that display the crossover discussed in the text. Note that in the figures, $t_0/U_0$ is the same as $T/J$ ratio in our notation. All solid curves are visual guides. (a) Entropy per degree-of-freedom, $\mathcal{S}(\mathcal{T} \to \infty)$ corresponds to a theoretical limit from a $\mathrm{SYK}_4$ model with no hopping terms. Inset: Specific heat (b) Thermal and electric resistivity.

$\rho \approx 1.12\ T/E_c$ which is linear in temperature and agrees with the expected slope from an analytical calculation in the $\mathrm{SYK}_4$ limit. In addition, it also recovers quadratic behavior in the low-temperature limit $T \ll E_c$. The numerical results from [17] are reproduced in Fig 6b. It is, however, troublesome that the slope of resistivity has an explicit dependence on $E_c$ and therefore $J$: it is not completely oblivious to the interaction strength unlike the Planckian metals we know from experiments [13].

Thus, we have an example of a higher-dimensional extension of SYK model with random hopping that shows linear-in-$T$ resistivity in an intermediate regime of temperatures $E_c \gg T$ and a crossover to Fermi liquid behavior at a characteristic scale $E_c$. The clean collapse of scaling and tractable numerics in this model highlight some of the best features of SYK models as candidates for a universal theory of strange metals.

### B. Landau levels in graphene flake with an irregular boundary

Next, we take a look at the question of whether the strong all-to-all random interactions which is the essence of SYK physics can be realised in a physical system. The authors

of [23] propose that it is the case in a graphene flake with an irregular boundary placed in a high magnetic field perpendicular to the flake. The key idea is the following: In the highly degenerate zeroth Landau level $\mathrm{LL}_0$ of a graphene flake, we can project the Coulomb interaction onto the $\mathrm{LL}_0$ wavefunctions which are sufficiently random given the irregularities in the boundary. Then, Coulomb interaction between the electrons populating $\mathrm{LL}_0$ resembles the $\mathrm{SYK}_4$ interaction term with complex fermions. In what follows, we explain this construction and its accompanying experimental considerations.

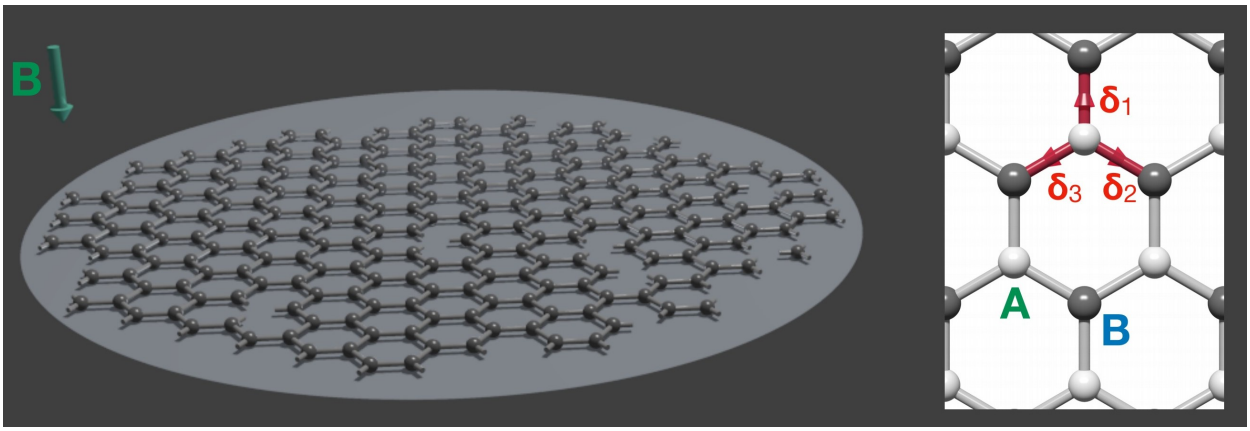


FIG. 7: **Graphene flake with irregular boundary in a magnetic field** Inset: Honeycomb lattice with sublattices A and B shaded as white and grey respectively. Also shown are the three nearest neighbor vectors $\delta_i$ between the sublattices. Figure from [23]

Consider a graphene flake (honeycomb lattice) with the non-interacting Hamiltonian with only nearest neighbor hopping

$$H_0^{NF} = -t \sum_{\substack{r,\delta \\ \sigma=\pm 1}} \left( a^\dagger_{r,\sigma} b_{r+\delta,\sigma} + b^\dagger_{r+\delta,\sigma} a_{r,\sigma} \right) \tag{34}$$

where $a^\dagger_\sigma$ and $b^\dagger_\sigma$ are the creation operators (for spin $\sigma$) on the sublattices A and B respectively and the vector $\delta$ goes from a site in A to a neighboring site in B (see inset in Fig 7). The effect of a magnetic field $\mathbf{B} = B\hat{z}$ on the tight-binding Hamiltonian is by a Peierls substitution and a Zeemann term

$$H_0 = -\sum_{\substack{\mathbf{r},\delta \\ \sigma=\pm 1}} t(\mathbf{r}, \mathbf{r}+\delta) \left( a^\dagger_{r,\sigma} b_{r+\delta,\sigma} + b^\dagger_{r+\delta,\sigma} a_{r,\sigma} \right) + \frac{g^* \mu_B B}{2} \sum_r (n_{\mathbf{r},\uparrow} - n_{\mathbf{r},\downarrow}) \tag{35}$$

where the hopping amplitude is $t(\mathbf{r}, \mathbf{r}+\delta) = t \, \exp(\frac{-ie}{\hbar c} \int_{\mathbf{r}}^{\mathbf{r}+\delta} \mathbf{A} \cdot d\mathbf{l})$. The non-interacting spectrum of the Hamiltonian with magnetic field is reorganized into Landau levels as usual,

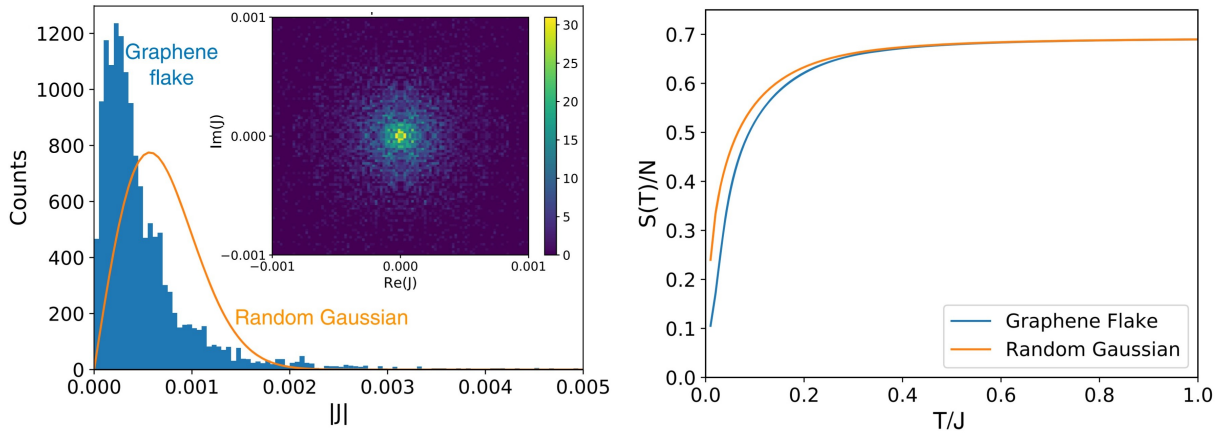


(a) (b)

FIG. 8: **Numerical verification of SYK physics**: (a) Probability distribution of the couplings $J_{ij;kl}$ calculated via Eq. (38) with a highly screened potential $V(r) = V_1 \sum_\delta \delta(r, \delta)$ vs a random Gaussian with the same variance. (b) Entropy of the graphene flake compared to a finite $N$ SYK model. Figures from [23].

but with some edge modes coming from the irregular boundary. Under the presence of disorder that respects the chiral symmetry $\chi : (a_{\mathbf{r}}, b_{\mathbf{r}}) \to (-a_{\mathbf{r}}, b_{\mathbf{r}})$, $\mathrm{LL}_0$ remains well-defined as a zero-energy state. Moreover, it is $N$-fold degenerate where $N = \Phi/\Phi_0$ is the number of magnetic flux quanta through the graphene flake (due to the Aharanov-Casher theorem [24]). The Zeemann term shifts the energy levels for spin up and spin down electrons, and we assume the chemical potential to be such that all negative-energy Landau levels are filled and $\mathrm{LL}_0$ is partially filled for one spin species. Thus, we can drop the spin index hereon.

In this scenario, the authors propose that we can project the Coulomb interaction onto the states in $\mathrm{LL}_0$. Consider a screened Coulomb interaction

$$H_{\mathrm{int}} = \frac{1}{2} \sum_{\mathbf{r},\mathbf{r'}} n_{\mathbf{r}} V(\mathbf{r} - \mathbf{r}') n_{\mathbf{r}'} \tag{36}$$

where the position indices run over all possible pairs of sites. Writing this in the basis of wavefunctions constituting $\mathrm{LL}_0$ $\phi_i(\mathbf{r})$,

$$H_{\mathrm{int}} = \sum_{i,j,k,l} J_{ij;kl}\ c_i^\dagger c_j^\dagger c_k c_l \tag{37}$$

with

$$J_{ij;kl} = \frac{1}{2} \sum_{\mathbf{r},\mathbf{r}'} (\phi_i(\mathbf{r})\phi_j(\mathbf{r}'))^* V(\mathbf{r} - \mathbf{r}')(\phi_k(\mathbf{r})\phi_l(\mathbf{r}')). \tag{38}$$

It can be argued that the couplings $J_{ij;kl}$ are random given the strongly disordered boundary and its resulting effect on $\phi_i(\mathbf{r})$. The authors of [23] explicitly check this by various numerical methods:

- the probability distribution of $J_{ij;kl}$ obtained by numerically diagonalizing a random graphene flake with $\sim 1950$ lattice sites looks approximately like a random Gaussian (Fig 8a),
- the entropy calculated for this graphene flake matches calculations for $\mathrm{SYK}_4$ with finite-$N$ (Fig 8b), and
- the level statistics $r_n = (E_{n+1} - E_n)/(E_n - E_{n-1})$ follow the expected behavior for different values of $N$.

Disorder that violates the chiral symmetry will generically be present in experimental samples, and can be modeled by a quadratic term among the $\mathrm{LL}_0$ levels

$$H_{\mathrm{dis}} = \sum_{ij} K_{ij} c_i^\dagger c_j. \tag{39}$$

This can come from next-to-nearest neighbor hopping or random onsite potentials. Hence, it would be desirable for the graphene flake to have a clean interior. As we have seen in Sec IV A, a quadratic term is relevant and will drive the system towards a Fermi liquid phase. While this can be controlled and the couplings $K_{ij}$ are expected to be small, it may be also essential to the physics of strange metals as we have discussed earlier.

The recipe for $N \approx 100$ degenerate states in the $\mathrm{LL}_0$ is to fabricate a graphene flake of dimension $L \approx 150$ nm at $B = 20T$ which is achievable in experiments. It is important to have a clean interior with an irregular boundary. Signatures of SYK physics may then be probed by measuring the differential tunneling conductance of the quantum dot $g(V) = dI/dV$ which measures the density of states and is known from theory to be $\sim 1/\sqrt{V}$ for small $V$ in $\mathrm{SYK}_4$ whereas $g(V) \sim$ const. in Fermi liquids.

## V. CONCLUSION

The SYK model has been the poster child of quantum holography since 2015. In this paper, we have summarised its significance in explaining the strange metal phase observed

in cuprates, cobaltates and ruthenates. First, we showed that the original SYK is a zero-dimensional exactly solvable model in the large-$N$ limit with some interesting features such as nonexistent quasiparticles and extensive zero-temperature entropy. Then we reviewed a higher-dimensional extension of the $SYK_4$ Hamiltonian with random quadratic hopping between the SYK islands. By simple power counting one can see that it displays a crossover from the non-Fermi liquid $SYK_4$ phase to the heavy Fermi liquid $SYK_2$ phase which is verified by numerical calculations of entropy and resistivity. The crossover is important because certain strange metals show a return to $\sim T^2$ dependence at lower temperatures (compared to Debye temperature) and this model could explain linear-in-$T$ resistivity in those cases. Finally we looked at a proposed experimental realization of the SYK quantum dot in a graphene flake. The $SYK_4$ interaction term is found to arise in a flake with a highly irregular boundary placed in a magnetic field and a partially filled zeroth Landau level so that the low energy physics is dominated by the degenerate states with zero energy. Projecting Coulomb interaction onto the random Landau level wavefunctions yields a sufficiently random interaction term that is then verified by numerics to be indeed of the form of $SYK_4$ with finite $N$.

Thus, what started out as a model to study spin-glasses, and later holography, has proved to be extremely relevant for studying a phase arising in the vocabulary of high-$T_c$ superconductors. The obvious unanswered question in the field is whether SYK physics has a microscopic realization in a specific system we already know to be a strange metal. It could also be the case that the similarities are superficial (or emergent), in which case the job would be to explain where the surprising similarities come from in the first place. In either case, solving the puzzle of strange metals will constitute a major achievement in condensed matter physics.

## ACKNOWLEDGMENTS

This work was undertaken in partial fulfillment of my candidacy exam. I am thankful to my advisor, Prof Ilya Gruzberg for picking such an interesting topic that helped me explore vital questions in condensed matter physics. I thank him for the continuing support at every step of my literature review. I also thank my committee members Prof Yuanming Lu, Prof Samir Mathur and Prof Marc Bockrath. I would also like to thank my colleague, Nishchhal

Verma for useful discussions on strange metal phenomenology.

---


[1] S. Sachdev and J. Ye, Gapless spin-fluid ground state in a random quantum Heisenberg magnet, Phys. Rev. Lett. **70**, 3339 (1993), arXiv:cond-mat/9212030 [cond-mat].

[2] A. Kitaev, A simple model for quantum holography, KITP Program: Entanglement in Strongly-Correlated Quantum Matter (2015).

[3] D. A. Trunin, Pedagogical introduction to SYK model and 2D Dilaton Gravity, arXiv e-prints , arXiv:2002.12187 (2020), arXiv:2002.12187 [hep-th].

[4] C. Proust and L. Taillefer, The remarkable underlying ground states of cuprate superconductors, Annual Review of Condensed Matter Physics **10**, 409 (2019), https://doi.org/10.1146/annurev-conmatphys-031218-013210.

[5] A. Abrikosov, *Fundamentals of the Theory of Metals* (Dover Publications, 2017).

[6] J. A. N. Bruin, H. Sakai, R. S. Perry, and A. P. Mackenzie, Similarity of scattering rates in metals showing T-linear resistivity, Science **339**, 804 (2013), https://science.sciencemag.org/content/339/6121/804.full.pdf.

[7] O. Gunnarsson, M. Calandra, and J. E. Han, Colloquium: Saturation of electrical resistivity, Rev. Mod. Phys. **75**, 1085 (2003).

[8] Y. Cao, D. Chowdhury, D. Rodan-Legrain, O. Rubies-Bigorda, K. Watanabe, T. Taniguchi, T. Senthil, and P. Jarillo-Herrero, Strange metal in Magic-Angle Graphene with near Planckian Dissipation, Phys. Rev. Lett. **124**, 076801 (2020).

[9] P. T. Brown, D. Mitra, E. Guardado-Sanchez, R. Nourafkan, A. Reymbaut, C.-D. Hébert, S. Bergeron, A.-M. S. Tremblay, J. Kokalj, D. A. Huse, and et al., Bad metallic transport in a cold atom Fermi-Hubbard system, Science **363**, 379–382 (2018).

[10] S.-D. Chen, M. Hashimoto, Y. He, D. Song, K.-J. Xu, J.-F. He, T. P. Devereaux, H. Eisaki, D.-H. Lu, J. Zaanen, and Z.-X. Shen, Incoherent strange metal sharply bounded by a critical doping in Bi-2212, Science **366**, 1099 (2019), https://science.sciencemag.org/content/366/6469/1099.full.pdf.

[11] A. Legros, S. Benhabib, W. Tabis, F. Laliberté, M. Dion, M. Lizaire, B. Vignolle, D. Vignolles, H. Raffy, Z. Z. Li, and et al., Universal T-linear resistivity and planckian dissipation in overdoped cuprates, Nature Physics **15**, 142–147 (2018).

[12] D. Chowdhury, Y. Werman, E. Berg, and T. Senthil, Translationally invariant Non-Fermi-Liquid metals with Critical Fermi Surfaces: Solvable models, Physical Review X **8**, 10.1103/physrevx.8.031024 (2018).

[13] R. Daou, N. Doiron-Leyraud, D. LeBoeuf, S. Y. Li, F. Laliberté, O. Cyr-Choinière, Y. J. Jo, L. Balicas, J.-Q. Yan, J.-S. Zhou, and et al., Linear temperature dependence of resistivity and change in the Fermi surface at the pseudogap critical point of a high-$T_c$ superconductor, Nature Physics **5**, 31–34 (2008).

[14] S. Martin, A. T. Fiory, R. M. Fleming, L. F. Schneemeyer, and J. V. Waszczak, Normal-state transport properties of $Bi_{2+x}Sr_{2-y}CuO_{6+\delta}$ crystals, Phys. Rev. B **41**, 846 (1990).

[15] J. Maldacena and D. Stanford, Remarks on the Sachdev-Ye-Kitaev model, Phys. Rev. D **94**, 106002 (2016).

[16] V. Bonzom, V. Nador, and A. Tanasa, Diagrammatic proof of the large N melonic dominance in the SYK model, Letters in Mathematical Physics **109**, 2611 (2019), arXiv:1808.10314 [math-ph].

[17] X.-Y. Song, C.-M. Jian, and L. Balents, Strongly Correlated Metal built from Sachdev-Ye-Kitaev models, Physical Review Letters **119**, 10.1103/physrevlett.119.216601 (2017).

[18] S. Sachdev, Bekenstein-Hawking entropy and Strange Metals, Phys. Rev. X **5**, 041025 (2015).

[19] Y. Gu, A. Kitaev, S. Sachdev, and G. Tarnopolsky, Notes on the complex Sachdev-Ye-Kitaev model, Journal of High Energy Physics **2020**, 10.1007/jhep02(2020)157 (2020).

[20] A. Altland and B. D. Simons, *Condensed Matter Field Theory*, 2nd ed. (Cambridge University Press, 2010).

[21] V. Rosenhaus, An introduction to the SYK model, Journal of Physics A: Mathematical and Theoretical **52**, 323001 (2019).

[22] Y. Gu, X.-L. Qi, and D. Stanford, Local criticality, diffusion and chaos in generalized Sachdev-Ye-Kitaev models, Journal of High Energy Physics **2017**, 10.1007/jhep05(2017)125 (2017).

[23] A. Chen, R. Ilan, F. de Juan, D. Pikulin, and M. Franz, Quantum holography in a graphene flake with an irregular boundary, Physical Review Letters **121**, 10.1103/physrevlett.121.036403 (2018).

[24] Y. Aharonov and A. Casher, Ground state of a spin-$\frac{1}{2}$ charged particle in a two-dimensional magnetic field, Phys. Rev. A **19**, 2461 (1979).